Stochastic qualifier of gel and glass transitions in laponite suspensions

F. Shayeganfar,[1] S. Jabbari-Farouji,[2] M. Sadegh Movahed,[3] G. R. Jafari,[3] and M. Reza Rahimi Tabar[1,4]
[1]*Department of Physics, Sharif University of Technology, P.O. Box 11365-9161, Tehran, Iran*
[2]*Le Laboratoire de Physique Theorique et Modeles Statistiques (LPTMS), Universite Paris-Sud, 91405 Orsay cedex, France*
[3]*Department of Physics, Shahid Beheshti University, G.C., Evin, Tehran 19839, Iran*
[4]*Fachbereich Physik, Universität Osnabrück, Barbarastraße, 49076 Osnabrück, Germany*
(Received 19 November 2009; revised manuscript received 27 April 2010; published 30 June 2010)

The existence of the important similarities between gelation and glass transition makes it hard to distinguish between the two types of nonergodic states experimentally. Here, we report on a stochastic analysis of the scattered light intensity through a colloidal particles suspension during the gel and glass formation. In this analysis, we exploit the methods developed for complex hierarchical systems, such as turbulence. Using the multiplicative log-normal cascade models, we provide a criterion to distinguish gels from glasses.

DOI: 10.1103/PhysRevE.81.061404 PACS number(s): 82.70.Dd, 02.50.Fz, 82.70.Gg

I. INTRODUCTION

Understanding the nature of disordered and nonequilibrium states of matter is of fundamental significance that has been an intense subject of research over the past few decades [1–13]. Gaining an insight into the structure of disordered states from both dynamic and static point of view has also direct practical implications. One of the main issues in the field is the distinction of gel and glassy states, which is still a matter of debate and demands further clarification despite the considerable amount of research going on in this area. The recent progresses in experimental manipulation techniques has promoted colloids as interesting model systems to elucidate the physics of various equilibrium and nonequilibrium physical phenomena including the glass formation and gelation.

Both gelation and glass formation can be considered as manifestations of the general Brownian motion in different regimes. Brownian motion is one of the most well known and fundamental of stochastic processes that has indeed come to occupy a central role in the theory and applications of stochastic processes. The displacement of a Brownian particle r with respect to its initial position at time t is a random stochastic variable that in the simplest case, obeys a Gaussian distribution with a zero mean. Colloidal particles having a size less than one micrometer undergo a random thermal Brownian motion in the dispersed fluid and their diffusion can be described by a general random walk. In the simplest case of dilute noninteracting spherical colloidal suspensions, the conditional probability distribution function of a single particle displacement follows the diffusion equation. However, for interacting colloidal particles, the diffusion of particles does not obey the simple diffusion equation anymore but can be described in the general framework of Smoluchowski equation [1]. For strongly enough interacting particles the diffusion of particles is slowed down as a result of interactions with neighboring particles. Depending on the strength and nature of interactions (repulsive/attractive) and volume fraction of particles then different types of disordered arrested states of matter are observed [4].

In repulsive colloidal systems as the particle volume fraction is increased, the particles become increasingly slower and for even higher volume fractions the glass transition is encountered [2]. On the other hand, colloidal gels are known to form at extremely low volume fractions $10^{-4}-10^{-2}$ in the presence of strong attractions [5] and of course in the intermediate regime where the repulsive and attractive interactions compete with each other a new state known as attractive glass emerges [4,14]. Gelation and the glass transition have important similarities. Both are ergodic to nonergodic transitions that are kinetic, rather than thermodynamic, in origin and distinguishing between these two types of nonergodic states experimentally is a long-standing controversy [7–11].

Laponite clay suspension modeled as a system of charged colloidal disks is an interesting system for which for both glass- and gel-like nonergodic states are reported [12–14]. The prominent feature of Laponite suspensions is their strong aging behavior, i.e., the evolution of the physical properties (diffusion, viscosity) of system with time elapsed since the sample preparation. Measuring the intensity correlations of scattered light from a large number of aging Laponite suspensions, one always observes two regimes of aging in the evolution of the intensity correlation functions. In the first regime the system is ergodic, whereas the second regime corresponds to a nonergodic arrested state. Changing the volume fraction in this system from very low values 10^{-3} to higher values 10^{-2}, first gel-like and then a glasslike ergodic to nonergodic transition is observed. Indeed changing the volume fraction, not only the number density of clay particles is changed but also the ionic strength which is a determining factor in electrostatic interaction is changed dramatically [14] leading to crossover from a gel state to a glass state.

Studying the aging dynamics of Laponite suspension from the ergodic regime to non-ergodic regime by light scattering Jabbari *et al.* provided direct criteria distinguishing gels from glasses [12,14]. Furthermore measuring the evolution of static structure factor of Laponite suspensions by means of small-angle x-ray scattering Ruzicka *et al.* provided another evidence of distinguishing between gel and glasses [13]. To summarize, the structure factor of glass state (high concentrations) is homogenous and changes very little with waiting time reminiscence of a frozen liquid but that of a gel state (low concentrations) is inhomogeneous and evolves with

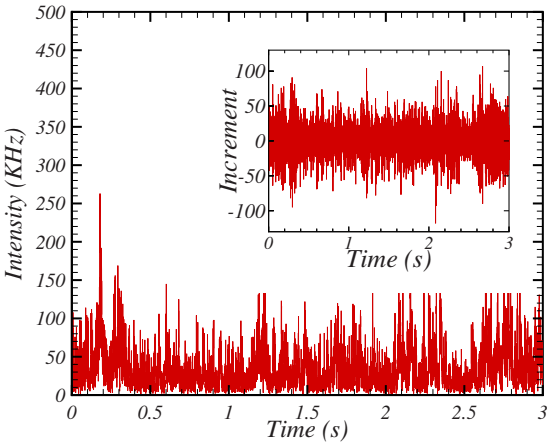

FIG. 1. (Color online) Intensity of light scattering during the gelation process. Inset: the time series for the $I(t+1)-I(t)$. In this paper, we express intensities in terms of the detector count rate in kHz.

time dramatically, suggesting formation of networklike structure or aggregation. From the dynamic point of view the diffusion of particles in gel and glass measured by dynamic light scattering behave very differently, although both show a nonexponential decay of correlation function which is a direct evidence of a non-Gaussian distribution of particles displacement. The short-time diffusion of particles in glass decreases only slightly while it drops significantly in a gel during the ergodic to nonergodic transition. The slow relaxation time of a glass grows exponentially with waiting time, while that of a gel grows faster than exponentially. Furthermore, the distribution of relaxation times is different between a gel and glass. A gel has a broad distribution, whereas a glass has a double-peaked broad distribution of relaxation times [12].

All these differences suggest that the random motion of particles in a glass intrinsically is different from that of a gel. Therefore, finding statistical tools that quantify these difference can provide us more insights and another direct method of distinguishing gels and glasses. The aim of this paper is to distinguish between gels and glasses by means of advanced stochastic analysis methods to analyze the time series of the scattered intensity during the gelation and glass formation, see Fig. 1 for a typical time series of the stochastic light intensity.

The time-dependent intensity of scattered light intensity is related to the fluctuating displacements of colloidal particles (the spatial Fourier transform of particles displacement) and reflects the instantaneous motion of them. Therefore, stochastic analysis of the time series of the scattered intensity can provide us with useful information about the nature of thermal random motion of Brownian particles. In the simplest case of dilute noninteracting particles, the scattered intensity time-series is a Markovian process with a Gaussian distribution. In a recent publication, we demonstrated that the fluctuations in the time series of the scattered intensity during the glass formation belong to this family of complex signals [15]. Using the multiplicative cascade model, Markovian method [16–20], and volatility correlations we showed that the light scattering intensity fluctuations from an aging glassy sample of Laponite shows a non-Gaussian character as expected and we provided methods for quantifying the deviations from the Gaussian process [15]. In this work, we have extended our previous study and have investigated the stochastic properties of light intensity fluctuations from different gel and glassy samples of Laponite as a function of waiting time using a robust method which is a type of cascade model [21–24].

Several cascade models have been proposed to model the experimental observations [22,23,25–27]. Castaing *et al.* proposed a multiplier method to model the probability density function (PDF) of a data set successive increments at different time scales [28]. This method is known also as log-normal cascade model and was introduced to study of fully developed turbulence [28,29]. However, it has been applied in diverse set of phenomena, such as solar and wind energies [30], foreign exchange rate [31], stock market index [32,33], human heartbeat fluctuations [34], and seismic time series [35].

The advantages of the cascade models are twofold. First, they provide a kernel to change the shape of probability distribution function from scale s to another scale s'. Second, they characterize the non-Gaussian shape of PDF with a so-called non-Gaussian parameter, here denoted as λ_s^2. We would like to note the readers that the non-Gaussian parameter λ_s^2 defined here is different from the conventional one which quantifies the deviations of the ratio of the fourth moment to 3 times the second moment of a stochastic variable from unity, sometimes also called flatness. The non-Gaussian parameter λ_s^2, captures the information from the whole shape of PDF, while the flatness only depends on second and fourth moments and does not include the complete information from the tails of PDF.

Our analysis of probability distribution function of the normalized scattered intensity shows that this distribution is non-Gaussian as expected and evolves with waiting time. The non-Gaussian parameter λ_s^2 extracted from the data grows with waiting time for both gel and glass samples. However, its rate of growth is different for gel and glass samples and the value of non-Gaussian parameter is smaller in gel samples, indicating the different nature of stochastic motion of colloids in gel and glass phase.

The paper is organized as follows: In Sec. II, we provide a brief review of the probability distribution function in the multiplicative cascade model. The sample preparation and experimental setup to record the intensity of light scattering are described in Sec. III. Application of the method to explore the stochastic nature of ergodic to nonergodic transition in colloidal suspensions is presented in Sec. IV. The last section is devoted to the discussion and concluding remarks.

II. MULTIPLICATIVE CASCADE MODELS: NON-GAUSSIAN PARAMETER

It has been shown that a non-Gaussian probability density function with fat tails can be represented by a stochastic multiplicative processes [28,36–40]. Suppose that $\{y(t)\}$ is a

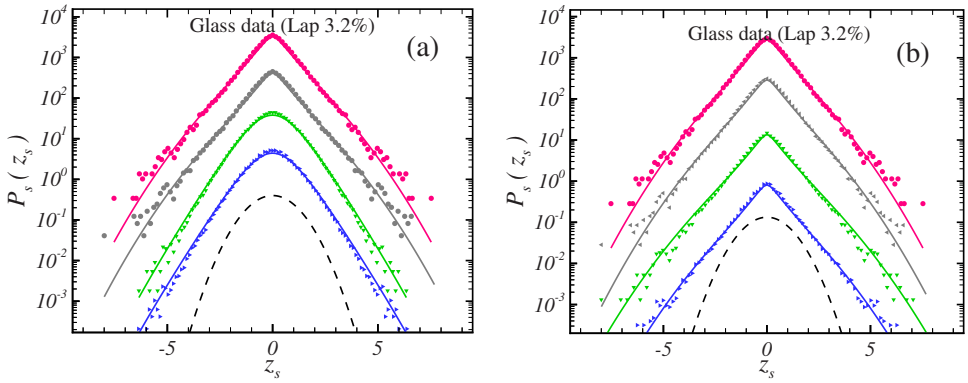

FIG. 2. (Color online) Continuous deformation of the increments' PDFs for the data sets (a) just after preparation of sample (t_w =80 min) in the low viscose phase and (b) during the appearance of viscoelastic phase (t_w=610 min) (here glass system) for s=5, 10, 20, and 40 ms (from top to bottom). Solid curves are the PDFs based on Eq. (3), while dashed curves are the Gaussian PDF. For clarity, the PDFs are shifted in the vertical directions.

time series and consider its increments as $Z_s(t)=y(t+s)-y(t)$. Let us define $z_s(t)=[Z_s(t)-\overline{Z_s}]/\sigma$, where $\overline{Z_s}$ and σ are the mean and variance of increments time series $Z_s(t)$.

In the cascade model one assumes that for a fixed t, the fluctuations at scales s and λs are related through the cascading rule,

$$z_{\lambda s}(t) = W_\lambda z_s(t), \quad \forall\, s,\ \lambda > 0, \tag{1}$$

where $\ln(W_\lambda)$ is a random variable. Iterating Eq. (1) forces implicitly the random variable W_λ to follow a log infinitely divisible law [41]. One of the simplest candidates for such processes is:

$$z_s(t) = \xi_s(t) e^{\omega_s(t)} \tag{2}$$

where $\xi_s(t)$ and $\omega_s(t)$ possess both independent Gaussian probability density function with zero mean and variance σ_s^2 and λ_s^2, respectively. Indeed the Eq. (2) was demonstrated to describe how the stochastic fluctuations evolve from large to small scales. The probability density function of increments $z_s(t)$ has been introduced by Castaing *et al.* [3], and it has the following expression,

$$P_s(z_s) = \int_0^\infty G_{\mathbf{s},\lambda_s}(\ln\sigma)\frac{1}{\sigma}F\left(\frac{z_s}{\sigma}\right)d(\ln\sigma). \tag{3}$$

where $G_{\mathbf{s},\lambda_s}$ is the self-similarity kernel and $P_s(z_s)$ converges to a Gaussian function when $\lambda_s \to 0$. In practical application to determine the scale-invariant behavior of probability density function of multiplicative processes, the non-Gaussian parameter λ_s^2 is estimated from common method of Bayesian statistics [42]. We introduce measurements and model parameters as $\{X\}:\{z\}$ and $\{\theta\}:\{\lambda_s,\sigma_s\}$, respectively. According to the Bayes theorem one has:

$$P(\lambda_s,\sigma_s|X) = \frac{\mathcal{L}(X|\lambda_s,\sigma_s)P(\lambda_s,\sigma_s)}{\int \mathcal{L}(X|\lambda_s,\sigma_s)d\lambda_s d\sigma_s}. \tag{4}$$

The first term in the nominator of r.h.s of the Eq. (4) is Likelihood and the second terms contains every initial information concerning model parameters, so-called prior distribution and expresses the degree of belief about the model. In the absence of every prior constraints, the posterior function, $P(\lambda_s,\sigma_s|X)$ is proportional to the Likelihood function. If there is no correlation between various measurements, consequently according to the central limit theorem, Likelihood function is given by a product of Gaussian functions as follows:

$$\mathcal{L}(X|\lambda_s,\sigma_s) = \exp\left[\frac{-\chi^2(\lambda_s,\sigma_s)}{2}\right]. \tag{5}$$

where χ^2 is defined by:

$$\chi^2(\lambda_s) = \int dz_s d\sigma_s \frac{[P_s(z_s) - P_{\text{castaing}}(z_s,\lambda_s,\sigma_s)]^2}{(\sigma^2_{\text{numeric}}(z_s) + \sigma^2_{\text{castaing}}(z_s,\lambda_s,\sigma_s))}. \tag{6}$$

Here $P_s(z_s)$ and $P_{\text{castaing}}(z_s,\lambda_s,\sigma_s)$ are PDFs computed directly from the data set and determined by Eq. (3), respectively. Also, σ_{numeric} is the mean standard deviation of $P_s(z_s)$ and σ_{castaing} is associated to probability density function derived by the left hand side of Eq. (3). Apparently, this Likelihood function to be maximum when for a value of the non-Gaussian parameter λ_s, χ^2 reaches to its global minimum. From computational point of view, marginalizing over the nuisance parameter, σ_s, may be taken too long, consequently to avoid this inconvenience, one can rewrite cascade model as:

$$P_s(z_s) = \int_0^\infty \frac{1}{\sqrt{2\pi\lambda_s^2}}\exp\left[-\frac{\ln^2(\sigma/\sigma_s)}{2\lambda_s^2}\right] \times \frac{1}{\sqrt{2\pi\sigma^2}}\exp\left(-\frac{z_s^2}{2\sigma^2}\right)d(\ln\sigma). \tag{7}$$

For a data set, $\{z\}$, with zero mean and unit variance, the left hand side of Eq. (7) has unit variance while the variance of the right hand side is $\sigma_1=\exp(\lambda_s^2)$. Therefore to have consistent equation one should choose $\sigma_s=\exp(-\lambda_s^2)$ [40].

We use data set with zero mean and unit variance through this paper to construct the cascade model. Therefore the Eq. (6) has just one free parameter and is modified as:

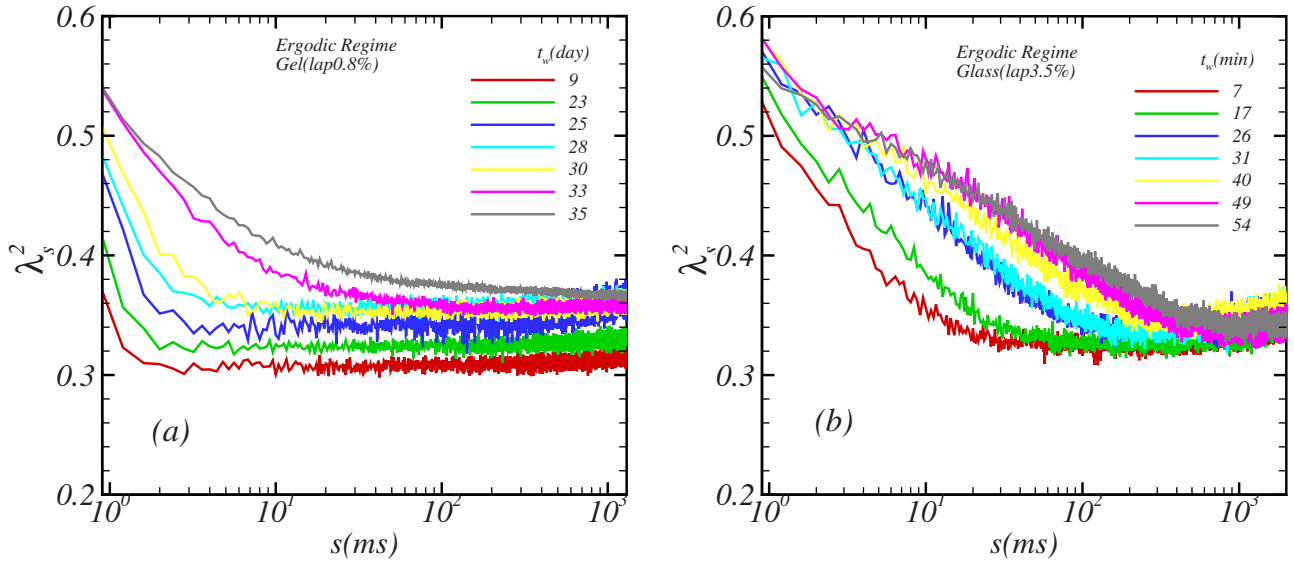

FIG. 3. (Color online) Scale dependence of λ_s^2 vs log s for ergodic regime, (a) gel samples and (b) glass samples.

$$\chi^2(\lambda_s) = \int dz_s \frac{[P_s(z_s) - P_{\text{castaing}}(z_s,\lambda_s)]^2}{(\sigma^2_{\text{numeric}}(z_s) + \sigma^2_{\text{castaing}}(z_s,\lambda_s))}. \quad (8)$$

Minimizing this χ^2 will give us the best Castaing parameter, λ_s^2 [28,43]. Recently it has been shown that the value of parameter λ_s^2 can be used as a precursor for extreme events such as earthquakes and crash of stock markets [32–35].

In the following, we will report the experimental setup and data preparation, and focus to explore time evolution of scattered light intensity from Laponite colloidal suspension. To detect the gel and glass transitions we use the Castaing parameter, λ_s^2 to investigate the temporal evolution of non-Gaussian parameter.

III. EXPERIMENTAL SETUP AND MEASUREMENTS

The Laponite grade used in this study was the Laponite XLG. We first dried it in an oven at 100 °C for one week and subsequently stored it in a desiccator to avoid moist adsorption from the air. We prepared a number of Laponite samples with different concentrations raning from 0.2 wt % to 3.6 wt %. Laponite solutions were prepared in ultra pure Millipore water (18.2 MΩ cm^{-1}) and stirred vigorously by a magnetic stirrer for one hour and a half to make sure that the Laponite particles are fully dispersed. Subsequently, the dispersions were filtered using Millipore Millex AA 0.8 μm filter units to obtain a reproducible initial state. This instant defines the zero of waiting time, $t_w=0$. A standard dynamic light scattering ($\lambda=632.8$ nm) measured the time-series of scattered intensity fluctuations at scattering wave vector $q = \frac{4\pi n}{\lambda}\sin(\frac{\theta}{2})$, in which $\theta=90°$ is the scattering angle. The intensity values were recorded every 406 μs.

IV. STOCHASTIC QUALIFIER OF THE GEL AND GLASS TRANSITIONS

We devote this section to the stochastic analysis of the time series of scattered light intensity from aging Laponite suspensions. When dissolved in water, Laponite spontaneously evolves from an initially ergodic liquidlike state to a nonergodic solidlike state. Therefore, two regimes of aging are observed: (i) the ergodic regime, where the measured time series is independent of position measured in the sample, (ii) the nonergodic regime where the measured time series depends on the position on the sample measured. In this regime, we measure an extra time series, in which we rotate the sample during the measurement and obtain the ensemble-averaged intensity. The transition from ergodic to nonergodic regime occurs at a certain time which we call ergodicity-breaking time and denote it as t_{eb}.

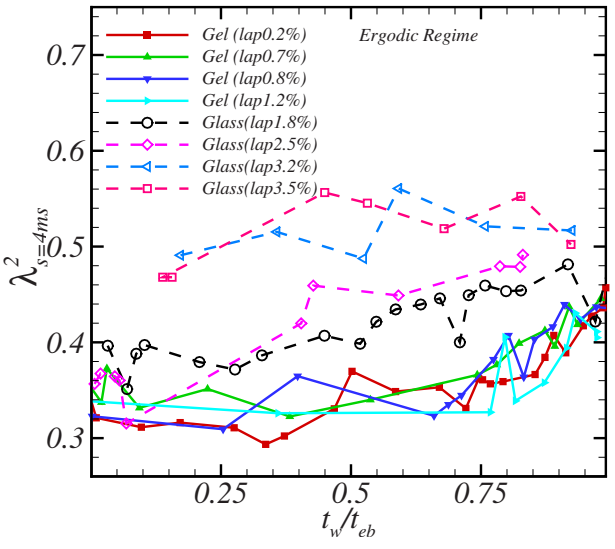

FIG. 4. (Color online) The local temporal dependence of λ_s^2 for various gel and glass samples in ergodic regime. Here, t_W and t_{eb} are waiting time and ergodic breaking time scales, respectively. The average value of λ_s^2 for glass samples are higher than its value for gel samples. It means that the PDF of light intensity increments has more deviation from Gaussian tails for glass samples.

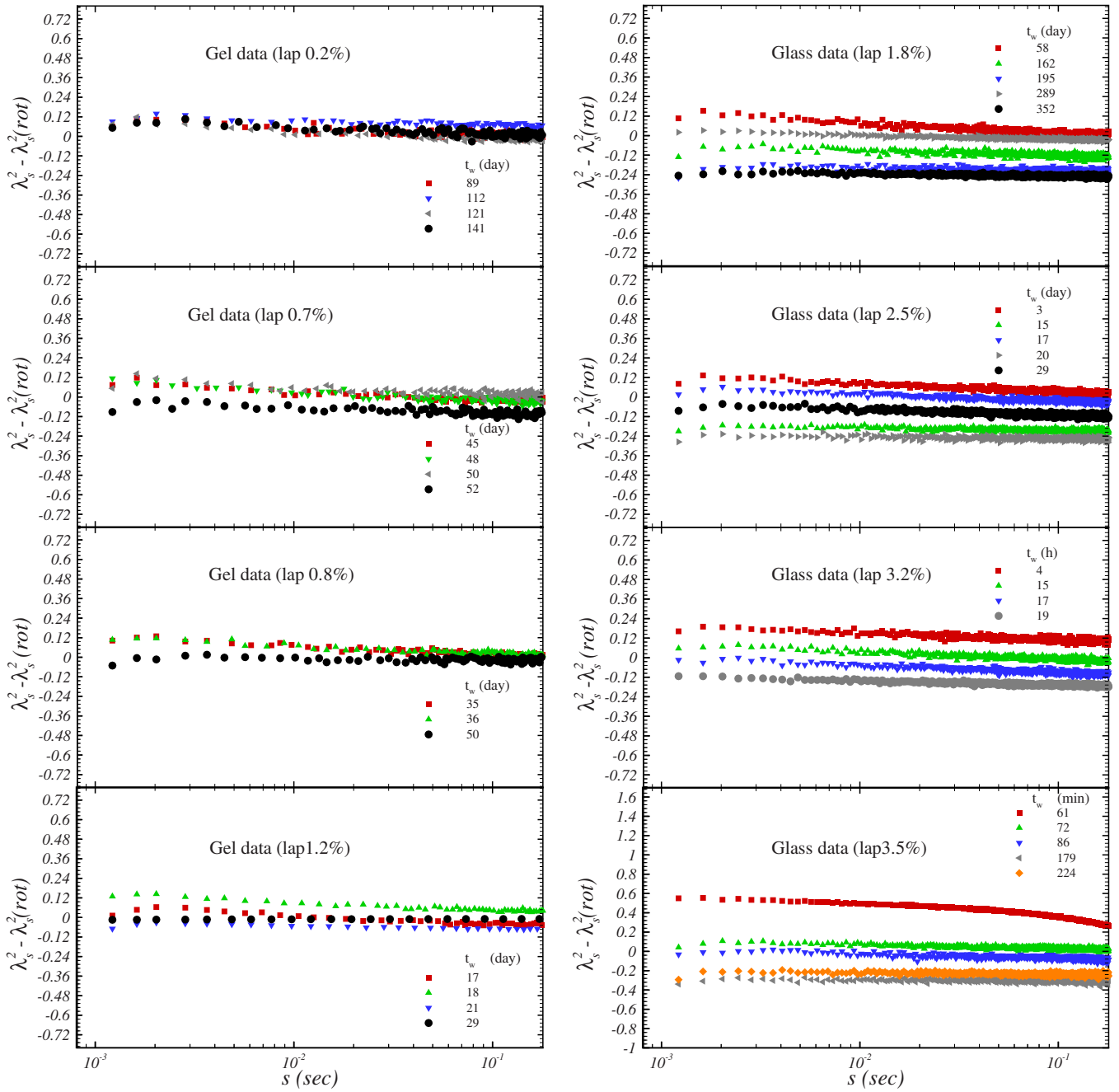

FIG. 5. (Color online) Scale-dependence of the subtracted fitting parameter for nonergodic regime (gel and glass samples), $\lambda_s^2 - \lambda_s^2(rot)$ of the Castaing parameter versus scale s for different waiting time t_w. They show that the values of parameter $\lambda_s^2 - \lambda_s^2(rot)$ for the gel systems are smaller than those for the glass systems.

We are interested in detecting the differences in the evolution of stochastic parameters during the ergodic to nonergodic transition in "gel" and "glass" states of Laponite colloidal suspension. Below, we describe in detail the method used for stochastic analysis of the data and the criterion obtained for distinguishing gels from glasses.

Let us consider the increment time series $\{y(i)\}$ as $y(i) = I(i+1) - I(i)$, where, $I(t)$ is the scattered light intensity at time t [see inset plot of Fig. 1]. We divide our data set into the semioverlapping subintervals $[1+s(k-1), s(k+1)]$, where s shows the value of scale used to construct data set and k is the index of the window of length $2s$. We use a first order polynomial function in order to remove the possible trends which may be presented in the underlying data for each scale, namely s [32,34]. The deviation from corresponding fitting function is given by $y_d(i)$. After detrending procedure a new data set on scale s, as $Z_s(i) = y_d(i+s) - y_d(i)$ is created. Here i runs from $1+s(k-1)$ to $s \times k$. As mentioned in the previous section for convenience, we rewrite time series as $z_s(t) = [Z_s(t) - \overline{Z_s}]/\sigma$, where σ and $\overline{Z_s}$ are the standard deviation and mean of data, respectively.

Now, we can obtain the PDF of normalized time series $z_s(t)$ directly from the data. Figure 2 shows PDFs of increment z_s for time scales just after preparation of sample t_w

=80 min in the low-viscose phase and at a later waiting time t_w=610 min, where the some viscoelastic properties are developed in the system. The sample has glass properties. One can see a continuous deformation of PDFs in various scales for the sample just after preparation [Fig. 2(a)]. While, after the ergodic to nonergodic transition PDFs are scale-invariant functions with respect to changing scale s [see Fig. 2(b)]. Solid curves are the PDFs based on Eq. (3) and the dashed curves are the Gaussian PDFs. We have found similar behavior for gel samples.

In the ergodic regime of aging, we have used the Eqs. (6) and (8) based on likelihood method to find λ_s^2 in terms of scale s. Figure 3 displays the scale-dependence of λ_s^2 for both gel and glass samples in the ergodic regime. We observe that for a given s, λ_s^2 increases with waiting time and for glass samples λ_s^2 is almost constant in the ergodic regime of aging for scales $s>1$ sec. To get a better insight into the evolution of the non-Gaussian parameter with waiting time, we have plotted λ_s^2 at a fixed scale, for instance s=4 ms, as a function of waiting time scaled with ergodicity-breaking time t_w/t_{eb} in Fig. 4.

According to Fig. 3, for s=4 ms, the difference between the values of λ_s^2 is large enough for ergodic and nonergodic regimes. Hence, such a time scale may be used as the characteristic time for the dynamics of the non-Gaussian indicator λ_s^2. Figures 4 clearly demonstrate a systematic increases of λ_s^2 for both gel and glass samples at this scale. From this figures, we notice that the average value of λ_s^2 for glass samples are higher than its value for the gel samples pointing to the fact that the PDF of light intensity increments shows a more pronounced deviation from Gaussian behavior for glass samples. Besides, this figure shows that the evolution of λ_s^2 is faster in glasses than gels, reflecting the different nature of particles diffusion in the two systems.

As we mentioned before, in the nonergodic regime of aging, we measure two time series. One which is measured at a specific point of the sample and one which is measured while rotating the sample to obtain the ensemble averaging for the nonergodic sample. We obtain the non-Gaussian parameter for each of these time series which we denote with λ_s^2 (specific point) and $\lambda_s^2(rot)$ (rotating sample time series) and then look at the difference of their values, i.e., $\lambda_s^2-\lambda_s^2(rot)$. In Fig. 5, we have displayed the scale-dependence of $\lambda_s^2-\lambda_s^2(rot)$ at different waiting times larger than ergodicity-breaking time. We find that the values of $\lambda_s^2-\lambda_s^2(rot)$ for the gel systems are systematically smaller than those for the glass systems and show a much weaker dependence on waiting time. Indeed its absolute values are almost zero for gel systems.

Also to distinguish the gel and glass phases, we have plotted the ensemble average of $\lambda_s^2-\lambda_s^2(rot)$ as a function of Laponite concentration in Fig. 6. It is defined as:

$$\langle \lambda_s^2 - \lambda_s^2(rot)\rangle = \frac{1}{\mathcal{N}(s_{\max}-s_{\min})}\sum_{i=1}^{\mathcal{N}}\sum_{s=s_{\min}}^{s_{\max}} \lambda_s^2 - \lambda_s^2(rot), \quad (9)$$

where $\mathcal{N}$ is the number of ensembles for each concentration. As clearly seen in Fig. 6, there are two separate regions related to gel and glass phases. Again the absolute values of $\langle \lambda_s^2-\lambda_s^2(rot)\rangle$ are almost zero for the gel systems.

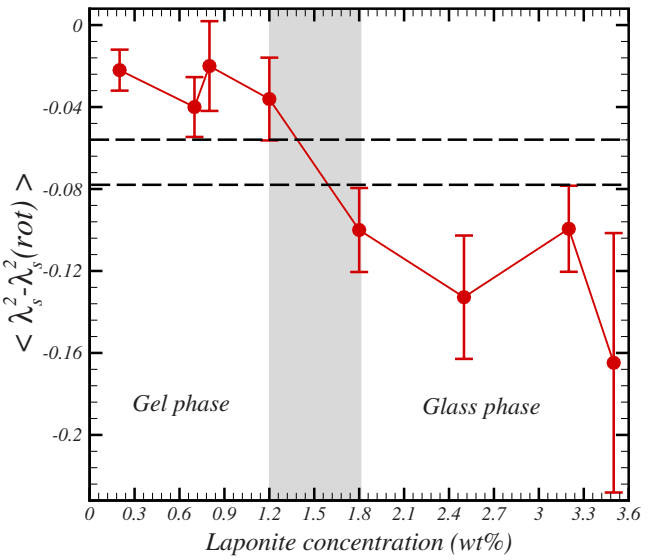

FIG. 6. (Color online) The ensemble average of $\langle \lambda_s^2-\lambda_s^2(rot)\rangle$ as a function of Laponite concentration.

V. DISCUSSION AND CONCLUSION

We have employed stochastic analysis methods based on cascade model to analyze the time series of scattered light intensity from aging Laponite suspensions. In this analysis, we have characterized the non-Gaussian nature of the light scattering intensity increments from aging gel and glassy samples by a non-Gaussian parameter λ_s^2 and show that this parameter behaves differently for gel and glass samples. Therefore, it can be employed as a criterion for distinguishing the gel transition from the glass transition. We find that in both ergodic and nonergodic regimes of aging, the non-Gaussian parameter is larger for the glassy samples compared to that of gel samples. Furthermore, we find that the non-Gaussian parameter grows with waiting time for both gel and glass samples in the ergodic regime. In the nonergodic regime, the non-Gaussian parameter remains mainly constant for the gel samples while it keeps on growing for glassy samples. This points to the different nature of gel and glassy samples and different types of mechanisms responsible for the aging of gel and glass. In a glass, the motion of particles is slowed down because particles are trapped in cages formed by their neighboring particles whereas in a gel the slowing down of motion of particle is due to formation of some sort of structure (network-like or aggregates) within the system. These findings are also in accord with the previous observation [12,13] in which the deviation from Gaussian behavior are quantified by the stretching exponent of stretched exponential function used to fit the correlation functions of light intensity. There, also one obtains a larger stretch exponent for glassy samples. We would like clarify that in our work the non-Gaussian parameter shows different behavior for the gel and the glass transitions of Laponite suspensions which occur at different densities. However, we believe that our method is also applicable to distinguish the gel and glass transition happening at the same density, work in this direction is on the way.

[1] J. K. G. Dhont, *An Introduction to Dynamics of Colloids* (Elsevier Science, New York, 1996).

[2] P. N. Pusey and W. van Megen, Phys. Rev. Lett. **59**, 2083 (1987); W. van Megen, S. M. Underwood, and P. N. Pusey, *ibid.* **67**, 1586 (1991).

[3] K. N. Pham *et al.*, Science **296**, 104 (2002); K. Kroy, M. E. Cates, and W. C. K. Poon, Phys. Rev. Lett. **92**, 148302 (2004).

[4] K. N. Pham, S. U. Egelhaaf, P. N. Pusey, and W. C. K. Poon, Phys. Rev. E **69**, 011503 (2004).

[5] D. A. Weitz, J. S. Huang, M. Y. Lin, and J. Sung, Phys. Rev. Lett. **54**, 1416 (1985); M. Carpineti and M. Giglio, *ibid.* **68**, 3327 (1992); P. N. Segrè, V. Prasad, A. B. Schofield, and D. A. Weitz, *ibid.* **86**, 6042 (2001).

[6] M. Kroon, G. H. Wegdam, and R. Sprik, Phys. Rev. E **54**, 6541 (1996).

[7] A. Mourchid, A. Delville, J. Lambard, E. Lecolier, and P. Levitz, Langmuir **11**, 1942 (1995).

[8] H. Tanaka, J. Meunier, and D. Bonn, Phys. Rev. E **69**, 031404 (2004).

[9] H. Tanaka, S. Jabbari-Farouji, J. Meunier, and D. Bonn, Phys. Rev. E **71**, 021402 (2005).

[10] P. Mongondry, J. F. Tassin, and T. Nicolai, J. Colloid Interface Sci. **283**, 397 (2005).

[11] D. Bonn, H. Kellay, H. Tanaka, G. Wegdam, and J. Meunier, Langmuir **15**, 7534 (1999).

[12] S. Jabbari-Farouji, G. H. Wegdam, and D. Bonn, Phys. Rev. Lett. **99**, 065701 (2007).

[13] B. Ruzicka, L. Zulian, R. Angelini, M. Sztucki, A. Moussaid, and G. Ruocco, Phys. Rev. E **77**, 020402(R) (2008).

[14] S. Jabbari-Farouji, H. Tanaka, G. H. Wegdam, and D. Bonn, Phys. Rev. E **78**, 061405 (2008).

[15] F. Shayeganfar, S. Jabbari-Farouji, M. S. Movahed, G. R. Jafari, and M. R. Tabar, Phys. Rev. E **80**, 061126 (2009).

[16] R. Friedrich, J. Peinke, and M. Reza Rahimi Tabar, *Encyclopedia of Complexity and Systems Science, 3574* (Springer, Berlin, 2009).

[17] G. R. Jafari, S. M. Fazeli, F. Ghasemi, S. M. Vaez Allaei, M. R. Tabar, A. Iraji Zad, and G. Kavei, Phys. Rev. Lett. **91**, 226101 (2003).

[18] F. Ghasemi, J. Peinke, M. Sahimi, and M. Reza Rahimi Tabar, Eur. Phys. J. B **47**, 411 (2005).

[19] P. Sangpour, G. R. Jafari, O. Akhavan, A. Z. Moshfegh, and M. R. Tabar, Phys. Rev. B **71**, 155423 (2005).

[20] F. Ghasemi, M. Sahimi, J. Peinke, R. Friedrich, G. R. Jafari, and M. R. Tabar, Phys. Rev. E **75**, 060102(R) (2007).

[21] T. C. Halsey, M. H. Jensen, L. P. Kadanoff, I. Procaccia, and B. I. Shraiman, Phys. Rev. A **33**, 1141 (1986).

[22] G. Paladin and A. Vulpiani, Phys. Rep. **156**, 147 (1987).

[23] C. Meneveau and K. R. Sreenivasan, J. Fluid Mech. **224**, 429 (1991).

[24] H. G. E. Hentschel, Phys. Rev. E **50**, 243 (1994).

[25] B. B. Mandelbrot, J. Fluid Mech. **62**, 331 (1974).

[26] E. A. Novikov, Phys. Fluids A **2**, 814 (1990); Phys. Rev. E **50**, R3303 (1994).

[27] U. Frisch, *Turbulence* (Cambridge University Press, Cambridge, England, 1995).

[28] B. Castaing, Y. Gagne, and E. J. Hopfinger, Physica D **46**, 177 (1990).

[29] B. Chabaud, A. Naert, J. Peinke, F. Chilla, B. Castaing, and B. Hebral, Phys. Rev. Lett. **73**, 3227 (1994).

[30] L. Sorriso-Valvo, V. Carbone, P. Veltri, G. Consolini, and R. Bruno, Geophys. Res. Lett. **26**, 1801 (1999).

[31] S. Ghashghaie, W. Breymann, J. Peinke, P. Talkner, and Y. Dodge, Nature (London) **381**, 767 (1996).

[32] K. Kiyono, Z. R. Struzik, and Y. Yamamoto, Phys. Rev. Lett. **96**, 068701 (2006).

[33] G. R. Jafari, M. S. Movahed, P. Noroozzadeh, A. Bahraminasab, M. Sahimi, F. Ghasemi, and M. Reza Rahimi Tabar, Int. J. Mod. Phys. C **18**, 11 (2007).

[34] K. Kiyono, Z. R. Struzik, N. Aoyagi, S. Sakata, J. Hayano, and Y. Yamamoto, Phys. Rev. Lett. **93**, 178103 (2004); K. Kiyono, Z. R. Struzik, N. Aoyagi, F. Togo, and Y. Yamamoto, *ibid.* **95**, 058101 (2005).

[35] P. Manshour, S. Saberi, M. Sahimi, J. Peinke, A. F. Pacheco, and M. R. Rahimi Tabar, Phys. Rev. Lett. **102**, 014101 (2009).

[36] H. Takayasu, A. H. Sato, and M. Takayasu, Phys. Rev. Lett. **79**, 966 (1997).

[37] U. Frisch and D. Sornette, J. Phys. (France) **7**, 1155 (1997).

[38] E. Bacry, J. Delour, and J. F. Muzy, Phys. Rev. E **64**, 026103 (2001).

[39] K. Lindenberg and B. J. West, *The Nonequilibrium Statistical Mechanics of Open and Closed Systems* (Wiley, New York, 1990).

[40] K. Kiyono, Z. R. Struzik, and Y. Yamamoto, Phys. Rev. E **76**, 041113 (2007).

[41] B. Dubrulle, Phys. Rev. Lett. **73**, 959 (1994); Z.-S. She and E. C. Waymire, *ibid.* **74**, 262 (1995).

[42] R. Colistete, Jr., J. C. Fabris, S. V. B. Gonçalves, and P. E. de Souza, Int. J. Mod. Phys. D **13**, 669 (2004).

[43] C. Beck, EPL **64**, 151 (2003).